Multi-view Feature Selection with Reinforcement Learning for EEG-based Automated ESES Diagnosis

Zhipeng He[1] (hezhp25@mail2.sysu.edu.cn), Yuxuan Li[1] (liyx577@mail2.sysu.edu.cn), Shishi Tang[1] (tangshsh9@mail2.sysu.edu.cn), Xinxin Peng[2](pengxx99@outlook.com), Rui Yang[1] (yangr83@mail2.sysu.edu.cn), Xuanhao Qi[1] (qixh5@mail2.sysu.edu.cn), Ziyi Chen[2*](chenziyi@mail.sysu.edu.cn), Yi Zhou[1*](zhouyi@mail.sysu.edu.cn)
[1] Zhongshan School of Medicine, Sun Yat-sen University, Guangzhou, China
[2] First Affiliated Hospital, Sun Yat-sen University, Guangzhou, China

Abstract

Electrical status epilepticus during sleep (ESES) is a serious condition that causes notable cognitive decline. It is characterized by distinct spike and slow-wave patterns on electroencephalograms (EEG). Clinical ESES diagnosis is extremely time-consuming and labor-intensive as it demands clinicians to manually interpret and count EEG screens. Existing automated diagnosis algorithms for ESES have major flaws, like struggling to adapt to complex spike and slow-wave patterns and not fully exploiting the rich multi-view features of EEG. To overcome these issues, we propose a multi-view feature selection framework integrating reinforcement learning and attention mechanisms for automated ESES diagnosis. A CLEAN reward mechanism is introduced to address complex multi-objective feature selection challenges. Experiments on the clinical data consisting of 36 epilepsy patients prove the proposed method's remarkable spike and slow-wave identification ability and high agreement with expert diagnoses. Our approach represents a significant step toward developing automated bedside ESES clinical diagnostic systems.

Keywords: Electrical status epilepticus during sleep (ESES); electroencephalograms (EEG); epilepsy; cognitive decline; automated diagnosis

Introduction

Epilepsy is a chronic brain disorder characterized by recurrent and transient episodes caused by abnormal neuronal discharges in the brain (Kandar, Das, Ghosh, & Gupta, 2012). Electrical status epilepticus during sleep (ESES) represents a unique electroencephalograms (EEG) phenomenon during the interictal phase in children with epilepsy, characterized by continuous or near-continuous epileptiform discharges during non-rapid eye movement (NREM) sleep, affecting either one or both sides of the brain (Loddenkemper, Fernández, & Peters, 2011). ESES is associated with the development of neurocognitive disorders (Smith & Hoeppner, 2003). It disrupts the local slow-wave activity at the epileptic focus, affects brain metabolism, and leads to localized plasticity impairments and neurological dysfunctions (Horvath, Csernus, Lality, Kaminski, & Kamondi, 2020).

ESES is characterized by specific EEG patterns of continuous spike and slow-waves, along with other complex waveforms. Quantifying these EEG patterns is crucial for the diagnosis of ESES. Clinically, the spike-wave index (SWI) during the slow-wave sleep is recognized as a diagnostic criterion for ESES. The SWI is defined as the ratio of the total duration of spike and slow-waves discharges to the NREM sleep time. A commonly accepted threshold for ESES diagnosis is an SWI more than 50% (Kulkarni, Albert, Klamer, Drees, & Twanow, 2023). Although the SWI provides a clear and quantifiable guideline for diagnosing ESES, the interpretation and calculation of spike and slow-waves during sleep stages still require visual inspection by medical experts, which remains a time-consuming and labor-intensive task for clinicians. Furthermore, the interpretation of spike and slow-waves and the final determination of ESES are subject to variability and subjectivity among the experts.

The spike and slow-waves identification can significantly enhance the efficiency of traditional ESES diagnosis, providing substantial clinical value. In recent years, researchers have made significant contributions to the automation of ESES diagnosis. Nonclercq et al. (Nonclercq et al., 2012) proposed an automatic spike detection algorithm based on a time-dependent k-means approach. This algorithm first clusters peak values and then uses the centroids of each cluster as templates to detect various spike types. The algorithm involves numerous threshold parameter settings at different stages, such as correlation and feature thresholds (e.g., rise-fall slopes and curvature), making it complex to operate. The template design often leads to reduced sensitivity due to the exclusion of atypical spikes. Zhou et al. (Zhou et al., 2022) developed a hybrid expert system integrating biogeography-based optimization with a morphology-based expert model. This approach incorporates personalized features and medical knowledge to mimic clinicians' decision-making in ESES quantification. However, the algorithm requires tuning multiple parameters, such as population size, crossover rate, and mutation rate. If set improperly, it can affect its performance. These automated algorithms for detecting ESES activity primarily rely on templates and morphological features, necessitating substantial expert knowledge. ESES is characterized by intense epileptic activity during slow-wave sleep, displaying a distinctive pattern of continuous spike and slow-waves discharges on EEG. The amplitude and duration of these characteristic waves vary significantly between different patients and even within the same patient over time. Additionally, there are often interleaved and overlapping spike and slow-waves (Topçu, Kılıç, Tekin, Aydın, & Turanlı, 2021; Wiwattanadittakul, Depositario-Cabacar, & Zelleke, 2020). Overall, existing methods struggle to adapt perfectly to these complex and variable conditions.

* Corresponding Authors

In D. Barner, N.R. Bramley, A. Ruggeri and C.M. Walker (Eds.), *Proceedings of the 47th Annual Conference of the Cognitive Science Society*

Although existing methods (Nonclercq et al., 2012; Zhou et al., 2022) have achieved acceptable accuracy in ESES diagnosis, they have not adequately addressed the following challenges: 1) These methods do not fully utilize the rich and multi-dimensional feature patterns inherent in EEG signals, making it difficult to adapt perfectly to the complex and variable nature of ESES. The features across different dimensions exhibit complementary characteristics. Constructing multi-view features from time, frequency, time-frequency, and nonlinear dynamics domains helps diagnostic method more comprehensively identify distinguishable characteristics of spike and slow-waves. 2) Not all of these multi-view features carry important information relevant to ESES diagnosis. Irrelevant and redundant features expand the feature space, making pattern detection more difficult and increasing the risk of overfitting. Feature selection is typically considered as an NP-hard problem, involving a search space with an exponential number of possible solutions based on the number of features (Mostafa, Ewees, Ghoniem, Abualigah, & Hashim, 2022; Zhang, Song, & Gong, 2017). Therefore, it is crucial to effectively select relevant features that significantly impact the performance of ESES diagnosis.

To the best of our knowledge, this is the first attempt to address the problem of estimating and selecting reliable brain activity information for EEG-based disease diagnosis by reinforcement learning framework. Overall, the main contributions of this paper are summarized below.

1) The framework constructs multi-views features using multi-domain from EEG signals within a unified framework. This utilizes the joint information from different views to achieve comprehensive information integration and classification. The complementary nature of different views provides rich brain activity information essential for ESES diagnosis tasks.

2) The feature selection challenge is modeled as a multi-agent coordination problem, with each feature corresponding to a learning agent, enabling independent determination of feature inclusion in the final subset. Agents decide feature inclusion, guided by a CLEAN-enhanced global reward. And an attention mechanism is integrated into the unified framework to capture feature interdependencies, ultimately improving the overall effectiveness of feature selection.

3) We conducted both the subject-dependent and subject-independent assessment experiments. Results indicate that the proposed method achieves superior performance compared to other feature selection methods. Ablation studies were also conducted to evaluate the impact of each component of the proposed method on performance.

Methodology

Problem definitions and notations

In the clinical ESES diagnosis, the proportion of spike and slow-waves in NREM sleep is usually described as SWI and is often used as an important reference standard for ESES diagnosis. We now detail the ESES diagnosis based on spike and slow-wave recognition problem based on EEG data.

Given the sequence of EEG signals $x=\{x_1,\cdots,x_i\}\in\mathbb{R}^{C\times T}$, where C and T of the matrix represent the number of channels and timepoints, respectively. x_i denotes the vector collected at the point i in time. Each second of the EEG signal for each patient was marked by an experienced professional physician. Suppose that the location of the pointed spike and slow-wave event in the marker segment is $Y_i \in [label_0, label_1]$. When $Y_i == label_1$ indicates that window i is spike and slow-waves, $Y_i == label_0$ indicates that window i is all non-spike and slow-waves EEG signals.

The automated quantification of EEG patterns related to ESES is achieved by spike and slow-waves and employing a key quantification parameter SWI. Thus, the goal of our proposed method is to automatically detect the number and duration of spike and slow-waves discharge data segments, and then calculate the SWI to ESES diagnosis. The SWI is defined as the total duration of all spike and slow-waves discharges divided by the total duration of the NREM phase during sleep. SWI is constructed as follows

$$\mathrm{SWI} = \frac{N\times L}{T_d} = \frac{\sum_{i=0}^{T_d} 1(if\ Y_i == label_1)}{T_d} \quad (1)$$

where N denotes the number of spike and slow-waves segments during NREM periods, L indicates the length of each spike and slow-waves segment, and T_d represents the duration of NREM periods. Fragments of signals classified as spike and slow-waves ($Y_i == label_1$) are summed and counted for the entire NREM sleep period.

Overall Framework

We construct a framework for ESES diagnosis based on EEG, as shown in figure 1. Specifically, it includes two core stages: the multi-view feature generation and embedding stage and reinforcement learning combined with attention stage.

As a highly complex nonlinear signal, the EEG signal uses the raw data as an input to the model, and the end result is often unsatisfactory. The usual practice is to perform an appropriate feature extraction of the raw data. In order to make full use of the multi-domain nature of EEG signal features and solve the problem of the lack of information of a single view, we combine the time, frequency, time-frequency domain and nonlinear dynamics to form multi-view features. Specifically, the EEG signal was recorded and segmented into different temporal segments. Multi-view features are extracted from the segmented EEG signals to form feature maps under different domain, and the extracted feature maps f_n are stitched together and transformed to form multiple feature representation.

However, the multi-view representations $\{V_1^t, V_2^t, \dots, V_n^t\}$ have the problems of information redundancy and dimension disaster, so we use the joint attention mechanism and reinforcement learning for feature selection. Figure1(b) shows the process of feature selecting. Combining environmental information in reinforcement learning, agents make action based on the current state S_t and observation O_t, and select features for processing (selection or rejection). The agents communicate, and their observations are integrated to obtain shared observations O_s^t. The state transfer is made through the ϵ-greedy policy, and the agent updates the state according to

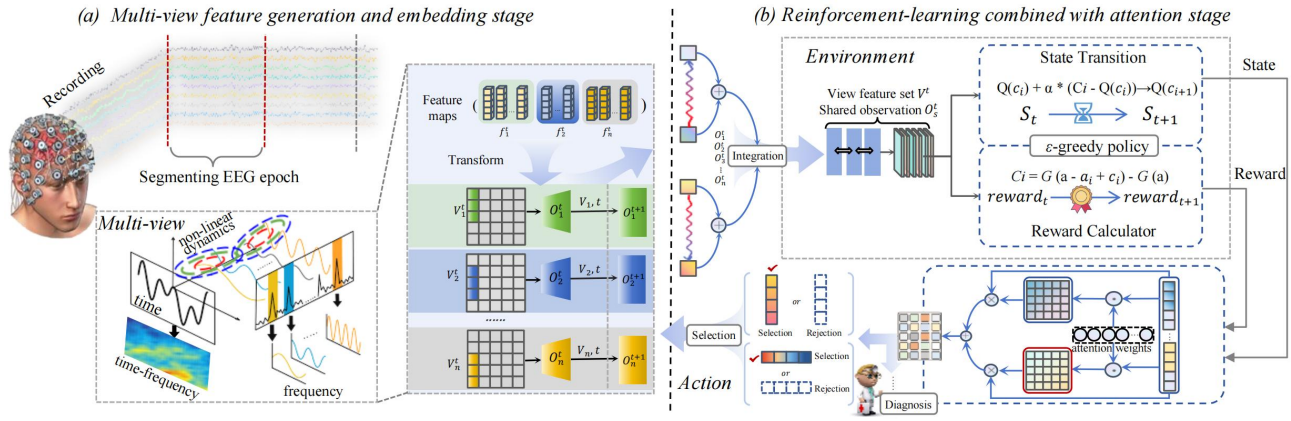

Figure 1: The framework of our proposed multi-view feature selection with reinforcement learning and attention. (a) Multi-view feature generation and embedding stage. (b) Reinforcement-learning combined with attention stage.

the current Q-value. The agent calculates the reward C_i based on the selected feature and the current state S_t, and the reward function G is used to evaluate the validity of the selection. During feature selection, the attention mechanism is used to weight the importance of different features, helping the agent to better focus on key features. The agents combine the calculated rewards and attention weights to select or reject features and incrementally learn the attentive selection over episodes. Based on the gained information, a decision is made to either start the next round $t + 1$ of feature selection or make a classification diagnosis.

Multi-view feature extraction

EEG signals, generated by synchronized neuronal activities in the brain, are complex with diverse frequency components and waveforms. This complexity makes raw signals hard to interpret (Siuly, Li, & Zhang, 2016). Multi-view feature extraction transforms them into representative and discriminative feature vectors, enhancing classification accuracy and aiding diagnostic model building.

Multi-view pattern recognition tasks effectively utilize the independence of each view and the correlations among different views during the learning process. This approach often results in better modeling outcomes compared to models based on single-view data. For EEG signals, there are multiple distinct view representations available(C. Li, Bian, Zhao, Wang, & Schuller, 2024).

Time domain features effectively characterize signal temporal variations, though they do not easily reveal frequency components (Guerrero-Mosquera, Malanda Trigueros, Iriarte Franco, & Navia-Vazquez, 2010). Frequency domain features reveal the frequency characteristics and the amplitude of various frequency components, suitable for signals with periodic variations. Time-frequency domain features allow analysis of the intrinsic non-stationary states of EEG signals. Nonlinear dynamics features reflect the EEG signal's responses and variations due to external disturbances or internal interactions (Moulines & Verhelst, 1995). Consequently, this study integrates features from aforementioned views to construct an initial multi-view EEG feature set.

Feature extraction from time domain. EEG signals are a type of signal analysis, commonly characterized using statistical metrics. In this study, three types of time-domain features are extracted, including zero-crossing rate (Schirmer & Mporas, 2020), standard deviation (Pala, 2023) , and AR spectral features(Jarchi, Rodgers, Tarassenko, & Clifton, 2018).

Feature extraction in frequency domain. Differential entropy is a frequency-domain feature used to measure the uncertainty or information content based on the rate of change of the series or differential (Saravanan, Chandra, Upadhye, & Gurugopinath, 2021). We extract differential entropy features from five common EEG frequency bands: δ, θ, α, β, γ.

Feature extraction in time-frequency domain. In this study, empirical mode decomposition (EMD) is employed as the method for processing the time-frequency domain (Huang, Su, Kareem, & Liao, 2016).

Feature Extraction in nonlinear dynamics. Numerous studies (Brunton, Proctor, & Kutz, 2016; Deng, Tian, Chen, & Harris, 2018; Y. Li, Tang, Jiao, & Zhou, 2024) demonstrate that nonlinear features, such as the Hurst exponent, Lyapunov exponent, approximate entropy, sample entropy, and permutation entropy, perform well (Caesarendra & Tjahjowidodo, 2017). We also utilize these nonlinear dynamic features.

Reinforcement learning combined with attention

We formulate the multi-view feature selection problem in ESES diagnosis as a Markov decision process based on reinforcement learning. We propose that the agent learns through trial-and-error interactions with its environment, accepting or rejecting corresponding features to attain the optimal feature set that maximizes cumulative rewards. The proposed reinforcement learning framework optimizes the extracted multi-view feature set, represented as $Optimize(F) = \{F^{time}; F^{freq}; F^{time\_freq}; F^{nonliner}\}$. The detailed descriptions of the key components are provided below.

State and Observation. We define the environment based on multi-view features subspace in this paper. Then, we define N agents, with each agent corresponding to different feature. In this paper, state $s_t \in S$ is defined as the specific case of the environment at time t. State includes the selection

of the current feature, which features are accepted or rejected. This information helps the agent evaluate the effectiveness of current feature selection strategies. At each time step *t*, each agent *i* perceives an individual local observation o_t^i :{(f_1^i ,..., f_{t-1}^i), f_t^i }∈*O* from its corresponding domain of the feature set. f_t^i is the state of the features that the current agent concerns. Although observation and state are closely related, they are not identical. The state is a complete description of the environment, while observation is the partial perception of the state. The agent needs to infer states by observation to make the best decision.

Policy and action. Our study adopts an ϵ-greedy policy based on value functions for agent action selection to balance exploration and exploitation. It balances exploitation, where the agent picks the highest Q-value action for immediate rewards, and exploration, randomly choosing an action with probability ϵ to find better strategies.

During the initialization phase, the agent has no knowledge of the environment, so all actions appear equally viable. The agent selects the action with the highest Q-value with a probability of $1-\epsilon$ and chooses a random action with probability ϵ. Over time, ϵ is typically reduced gradually, meaning the agent shifts from exploring more to exploiting the known best strategies. This can be achieved by implementing a decay strategy.

$$\epsilon = \max(\epsilon_{\min}, \epsilon_{\text{init}} \times \text{decay\_rate}^{\text{step}}) \quad (2)$$

where $\epsilon_{\min}$ is the minimum value of ϵ, ϵ_{init} is the initial value of ϵ, decay_rate is the decay rate, and step represents the current episode number. By adjusting ϵ, the agent can explore more strategies in the early stages of learning and increasingly exploit the known best strategies in the later stages.

Additionally, an agent's exploratory actions can modify other agents' reward signals, even when they take greedy (i.e., optimal) actions. This noisy interference can disrupt the current agent's learning. To mitigate it and aid self-behavior identification, we use a CLEAN reward for better feature selection coordination and learning.

The core idea of the CLEAN reward is to provide each agent with a "CLEAN" individual reward signal. This signal is defined as the difference between the global reward when all agents take greedy actions and the global reward when the current agent takes an exploratory action. The calculation formula is as follows:

$$C_i = G(a - a_i + c_i) - G(a) \quad (3)$$

where C_i is the CLEAN reward for agent i, $G(a)$ is the global reward when all agents take greedy actions, and a represents the set of actions taken by all agents. And a_i, c_i are the current actions taken by agent i and the possible exploratory action.

The CLEAN reward C_i is used to update the Q-value of agent *i* for the exploratory action c_i. The update formula is as follows:

$$Q(c_{i+1}) \leftarrow Q(c_i) + \alpha(C_i - Q(c_i)) \quad (4)$$

where $Q(c_i)$ represents the Q-value of agent *i* for taking the exploratory action c_i. The term α is the learning rate, which determines the extent to which new information affects the Q-value.

In each episode, the process is repeated, enabling the agent to learn and adjust strategies according to the CLEAN reward. Agents can clearly identify features beneficial to classification and make better feature selection decisions.

Reward. The reward function is a critical factor in an agent's decision-making process. The reward function defines the feedback an agent receives from the environment after executing an action. This feedback is quantified to evaluate whether the agent's action is good or bad. The design of the reward function directly impacts the agent's learning process and the formation of its final strategy. The reward function is defined based on the size of the feature subset and classification performance as follows:

$$\text{Reward} = \begin{cases} P, & if\ s \le k \\ \frac{P_k}{s}, & if\ s > k \end{cases} \quad (5)$$

where *k* represents the maximum allowed number of features, and *s* is the size of the current feature subset. If the feature subset size *s* is less than or equal to the upper limit *k*, the reward is given by the performance *P*. This means that if the agent selects a feature subset that meets the size requirement and maintains good classification performance, it receives a positive reward, encouraging the agent to continue selecting such subsets in the future. If *s*>*k*, the reward is $\frac{P_k}{s}$. If the size *s* of the feature subset exceeds the upper limit *k*, the reward obtained by the agent will decrease, specifically the $\frac{P_k}{s}$. This design aims to impose a penalty to reduce the likelihood of selecting overly large feature subsets, as such subsets can lead to overfitting or decreased computational efficiency.

The reward function encourages the agent to find a balance during feature selection, ensuring the subset maintains good classification performance while keeping the number of features under control. In this way, the agent learns over time to select feature subsets that are most beneficial to the diagnosis task while maintaining a moderate size.

Attention. In the attention-based module, firstly, the parameter W_{atten} of the attention layer is initialized. Subsequently, the inner product operation is carried out between the attentional weights and the *f* features chosen by reinforcement learning, expressed as α=<*f*, W_{atten}>. The softmax is then applied to these values, generating the updated attention weights $\alpha^*=softmax(\alpha)$. After obtaining the attention weights, we extract the updated feature vectors in the following way. The new feature vector *F* is calculated as a weighted sum of the original feature vectors, $F = \sum_j \alpha_j^* f_j$. Then, a fully connected layer is incorporated as a classifier.

Materials and Experiments

Datasets Collection and Processing

Patients. Patients undergoing long-range video EEG were collected. The EEG recordings were inspected by medical experts. Ultimately, a total of 36 epilepsy patients were

included in this study, consisting of 18 patients with ESES and 18 patients without ESES.

Data collecting. For each patient, 19 EEG electrodes are positioned according to the International 10-20 system, and continuous scalp EEG signals are being recorded over a 24-hour period using Nicolet EEG acquisition equipment. The spike and slow-waves as well as the ESES status of all patients in the experiment are annotated. The sleep stages are annotated as wake, NREM, and REM periods. Spike and slow-waves' annotations include the start timestamp and duration.

Experimental settings

We perform experiments as both subject-dependent and subject-independent and follow the experimental scenario setup provided in the previous work (Ko, Jeon, & Suk, 2020).

Subject-dependent (SD). The training set and the test set are divided according to the 5-fold cross-validation method. Each subject was divided into five mutually exclusive subsets of similar sizes. The method is then trained on four subsets and tested on the remaining subset.

Subject-independent (SI). The leave-one-out validation is adopted. The EEG of the target subjects are used as the test set, and the EEG of the remaining subjects are used as the training set. This approach helps to provide robust estimates of the generalization ability of our method.

Evaluation Criteria

SWI is the important criterion for the diagnosis of ESES. It was defined as the proportion of the total duration of spike and slow-waves to NREM duration. Thus, our method needs to validate the effect of quantified spike and slow-waves and then derive the diagnosis of patients with ESES.

The effective of spike and slow-waves identification. To evaluate the performance of our proposed method for spike and slow-waves identification, various evaluation indicators are used in this study including accuracy (ACC), true positive rate (TPR) and true negative rate (TNR).

Consistency of ESES diagnosis. The Kappa coefficient is used to assess the degree of agreement between the ESES diagnosis made by our proposed method and the physician's ESES diagnosis. Kappa value cloud provide a quantitative method to assess the consistency of diagnosis, helping to determine whether the proposed method is reliable and whether it can replace or assist manual diagnosis. The meanings corresponding to the kappa value within the range of 0-1 are as follows: 0~0.20: very low agreement (slight); 0.21~0.40: general agreement (fair); 0.41~0.60: moderate agreement (moderate); 0.61~0.80: high agreement (substantial); 0.81~1: almost complete agreement (almost perfect).

Result and Discussion

Quantitative evaluation

We present the quantitative results under the experimental setting of SD and SI evaluation in table 1-6. And table 1-6 also give the paired-sample t-test of our method and other modules or methods. Overall, our method outperformed the other comparison methods. The effectiveness of the key modules is explored and demonstrated through ablation study. Below, we discuss the relevant results in more detail.

Performance evaluation and ablation study. For the SD experiment, in terms of spike and slow-waves identification, our method obtains ACC of 94.84%, TPR of 94.31%, and TNR of 93.74%, respectively. On Consistency of ESES diagnosis, the kappa score of our proposed method up to 0.93, reaching the degree of almost perfect. For the SI experiment, in terms of spike and slow-waves identification, our method achieves ACC of 89.38%, TPR of 89.93%, and TNR of 89.61%. The average kappa is 0.87 in the consistency of ESES diagnosis, reaching almost complete agreement.

We conduct an ablation study to validate the effectiveness of each module in our proposed method. Our method is built upon multi-view features selection with attention-based reinforcement learning. The results of the ablation study show that the application of reinforcement learning contributed the most to the improvement of the diagnostic performance. The multi-view features, attention mechanism also have positive effects. Combining these parts simultaneously can maximize the effect of ESES diagnosis, as shown in table 1-6.

Table 1: Results on spike and slow-waves identification under the subject-dependent

Method	TPR(%)	TNR(%)	ACC(%)
time feature	84.14(17.27)**	92.89(10.71)~	87.76(13.41)**
frequency feature	90.39(9.69)*	94.93(7.79)~	91.21(9.28)*
time-frequency	83.29(17.24)**	87.82(15.21)*	82.57(13.96)**
nonlinear feature	84.67(13.40)**	93.39(9.08)~	87.25(11.26)*
All feature concate	88.47(14.34)*	95.33(7.59)~	90.13(13.47)*
w/o RL	89.11(13.02)*	90.46(3.56)*	90.94(10.89)*
w/o attention	90.21(10.12)*	91.56(8.38)~	92.07(9.30)~
Proposed (Ours)	94.31(11.42)	93.74(4.69)	94.84(7.38)

w/o indicates the removal of specific module
paired-sample t-test, ~p> 0.05, *p < 0.05, **p < 0.01

Table 2: Results on spike and slow-waves identification under the subject-independent

Method	TPR(%)	TNR(%)	ACC (%)
time feature	51.92(50.04)**	72.10(28.70)**	58.71(27.55)**
frequency feature	82.41(36.67)*	90.14(12.11)~	81.11(19.81)*
time-frequency	67.10(31.30)**	81.43(24.71)**	69.12(13.97)**
nonlinear feature	70.73(29.90)**	86.50(15.43)*	75.86(17.99)**
All feature concate	82.52(35.48)**	88.41(17.34)~	83.09(16.89)**
w/o RL	86.48(8.56)**	87.30(7.89)*	86.42(10.20)*
w/o attention	84.83(9.75)*	88.45(8.61)*	87.16(15.08)~
Proposed (Ours)	89.93(10.45)	89.61(9.21)	89.38(12.15)

w/o indicates the removal of specific module
paired-sample t-test, ~p> 0.05, *p < 0.05, **p < 0.01

Table 3: Results on consistency of ESES diagnosis under the subject-dependent

Method	Kappa	Consistency
time feature	0.83(0.18)**	almost perfect
frequency feature	0.89(0.15)*	almost perfect
time-frequency feature	0.78(0.20)**	substantial
nonlinear feature	0.78(0.20)**	substantial
All feature concate	0.86(0.12)*	almost perfect
w/o RL	0.89(0.13)*	almost perfect
w/o attention	0.91(0.14)~	almost perfect
Proposed (Ours)	0.93(0.15)	almost perfect

paired-sample t-test, ~p> 0.05, *P < 0.05, **P < 0.01

Table 4: Results on consistency of ESES diagnosis under the subject-independent

Method	Kappa	Consistency
time feature	0.11(0.24)**	slight
frequency feature	0.72(0.22)*	substantial
time-frequency feature	0.56(0.27)**	moderate
nonlinear feature	0.44(0.29)**	moderate
All feature concate	0.70(0.24)**	substantial
w/o RL	0.72(0.19)*	substantial
w/o attention	0.82(0.17)*	almost perfect
Proposed (Ours)	0.87(0.22)	almost perfect

paired-sample t-test, ~p> 0.05, *P < 0.05, **P < 0.01

Comparisons with other feature selection methods. For feature selection, we compare the performance of our proposed method against three types of typical competing feature selection methods in EEG research. No-feature selection is used as a baseline method. Minimal redundancy maximal-relevance (mRMR) based on Filtering algorithm, recursive feature elimination (RFE) based on the Wrappers algorithm, and Embedded-based lasso regression are used for comparison.

To effectively test the validity of the feature selection method, we set that all steps are the same, and the only difference is in the steps of feature selection. Table 5-6 summarize the results of several feature selection methods in the experimental setting of SD and SI evaluation. The first obvious observation is that using all features does not use any feature selection method with the worst performance, indicating the catastrophic nature of the dimensional problem. And our proposed feature selection method is able to select better and more differentiated features, which can achieve better performance.

Table 5: Performance of our method and other feature selection methods under the subject-dependent

Method	ACC (%)	Kappa	Consistency
Baseline	90.13(13.47)*	0.86(0.12)**	almost perfect
Filtering-mRMR	91.21(14.32)~	0.88(0.15)*	almost perfect
Wrapper-RFE	90.33(10.52)*	0.87(0.13)*	almost perfect
Embedded-lasso	92.49(14.45)~	0.87(0.18)*	almost perfect
Proposed (Ours)	94.84(7.38)	0.93(0.15)	almost perfect

paired-sample t-test, ~p> 0.05, *P < 0.05, **P < 0.01

Table 6: Performance of our proposed method and other feature selection methods under the subject-independent

Method	ACC (%)	Kappa	Consistency
Baseline	83.09(16.89)**	0.70(0.24)**	substantial
Filtering-mRMR	84.96(12.86)**	0.73(0.18)**	substantial
Wrapper-RFE	84.38(13.71)*	0.76(0.26)*	substantial
Embedded-lasso	85.21(16.23)*	0.71(0.16)**	substantial
Proposed (Ours)	89.38(12.15)	0.87(0.22)	almost perfect

paired-sample t-test, ~p> 0.05, *P < 0.05, **P < 0.01

Qualitative analysis

By analyzing the optimized selected features, the rationale and rationality of the proposed method can be understood. We visualize the activation representations of the optimized selected features on the brain topography map. Figure 2(a) and (b) show the brain activation status of the non-spike and slow-waves and spike and slow-waves in patients with ESES, respectively. Darker colors indicate higher weights assigned to the corresponding electrodes.

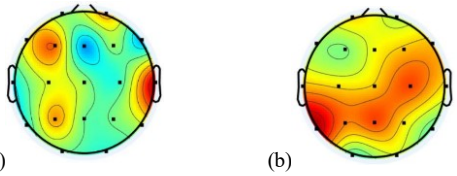

(a) (b)

Figure 2: (a) The brain activation status of the non-spike and slow-waves. (b) The brain activation status of the spike and slow-waves.

Obviously, it will be deeper around T3, C3, T5 and C4, which suggests the temporal and occipital region where abnormal discharges occur in patients with ESES. This is consistent with the clinical EEG findings of BECT patients with ESES (Panayiotopoulos, Michael, Sanders, Valeta, & Koutroumanidis, 2008). This finding also implies that the diagnostic approach we propose is explainable.

Conclusion

This paper introduces a novel multi-view feature selection method with reinforcement learning and attention for automated ESES diagnosis. The features of EEG signals are first generated from different views, and then multi-view features are selected by combining reinforcement learning and attention mechanisms. The feature representation can be effectively optimized, further enhancing the versatility of the method to achieve better ESES diagnosis across epilepsy patients. The experimental results indicate that the proposed method demonstrates good diagnostic capabilities for different patients as well as for the same patient at different times, showing a high level of consistency with physician diagnoses. Overall, the proposed method can help establish an accurate and efficient automated diagnosis system for patients with ESES, potentially enabling early treatment for patients.

Acknowledgments

This work was partly funded by the Key Research and Development Program of China (Grant 2022YFC3601600) , the National Natural Science Foundation of China (NSFC) (Grant 61876194), the Key Technologies Research and Development Program of Guangzhou Municipality (Grant 202206010028), the Province Natural Science Foundation of Guangdong, China (Grant 2024A1515011989 and 2025A1515012872), the Fundamental Research Funds for the Central Universities, Sun Yat-sen University (Grant 24xkjc025), and Graduate International Academic Exchange Program (Zhongshan School of Medicine) (Grant 50000-12251000).

References

Brunton, S. L., & Kutz, J. N. (2016). Discovering governing equations from data by sparse identification of nonlinear dynamical systems. *Proceedings of the national academy of sciences, 113*(15), 3932-3937.

Caesarendra, W., & Tjahjowidodo, T. (2017). A review of feature extraction methods in vibration-based condition monitoring and its application for degradation trend estimation of low-speed slew bearing. *Machines, 5*(4), 21.

Deng, X., Tian, X., Chen, S., & Harris, C. J. (2018). Deep principal component analysis based on layerwise feature extraction and its application to nonlinear process monitoring. *IEEE Transactions on Control Systems Technology, 27*(6), 2526-2540.

Guerrero-Mosquera, C., Malanda Trigueros, A., Iriarte Franco, J., & Navia-Vazquez, A. (2010). New feature extraction approach for epileptic EEG signal detection using time-frequency distributions. *Medical & biological engineering & computing, 48*, 321-330.

Horvath, A. A., Csernus, E. A., Lality, S., Kaminski, R. M., & Kamondi, A. (2020). Inhibiting epileptiform activity in cognitive disorders: possibilities for a novel therapeutic approach. *Frontiers in Neuroscience, 14*, 557416.

Huang, G., Su, Y., Kareem, A., & Liao, H. (2016). Time-frequency analysis of nonstationary process based on multivariate empirical mode decomposition. *Journal of Engineering Mechanics, 142*(1), 04015065.

Jarchi, D., Rodgers, S. J., Tarassenko, L., & Clifton, D. A. (2018). Accelerometry-based estimation of respiratory rate for post-intensive care patient monitoring. *IEEE Sensors Journal, 18*(12), 4981-4989.

Kandar, H., Das, S. K., Ghosh, L., & Gupta, B. K. (2012). Epilepsy and its management: A review. *Journal of PharmaSciTech, 1*(2), 20-26.

Ko, W., Jeon, E., & Suk, H.-I. (2020). A novel RL-assisted deep learning framework for task-informative signals selection and classification for spontaneous BCIs. *IEEE Transactions on Industrial Informatics, 18*(3), 1873-1882.

Kulkarni, N., Albert, D. V., Klamer, B., Drees, M., & Twanow, J. D. (2023). The Spike–Wave Index of the first 100 seconds of sleep can be a reliable scoring method for electrographic status epilepticus in sleep. *Journal of Clinical Neurophysiology, 40*(6), 547-552.

Li, C., Bian, N., Zhao, Z., Wang, H., & Schuller, B. W. (2024). Multi-view domain-adaptive representation learning for EEG-based emotion recognition. *Information Fusion, 104*, 102156.

Li, Y., Tang, B., Jiao, S., & Zhou, Y. (2024). Optimized multivariate multiscale slope entropy for nonlinear dynamic analysis of mechanical signals. *Chaos, Solitons & Fractals, 179*, 114436.

Loddenkemper, T., Fernández, I. S., & Peters, J. M. (2011). Continuous spike and waves during sleep and electrical status epilepticus in sleep. *Journal of Clinical Neurophysiology, 28*(2), 154-164.

Mostafa, R. R., Ewees, A. A., Ghoniem, R. M., Abualigah, L., & Hashim, F. A. (2022). Boosting chameleon swarm algorithm with consumption AEO operator for global optimization and feature selection. *Knowledge-Based Systems, 246*, 108743.

Moulines, E., & Verhelst, W. (1995). Time-domain and frequency-domain techniques for prosodic modification of speech. *Speech coding and synthesis*, 519-555.

Nonclercq, A., Foulon, M., Verheulpen, D., De Cock, C., Buzatu, M., Mathys, P., & Van Bogaert, P. (2012). Cluster-based spike detection algorithm adapts to interpatient and intrapatient variation in spike morphology. *Journal of neuroscience methods, 210*(2), 259-265.

Pala, O. (2023). A new objective weighting method based on robustness of ranking with standard deviation and correlation: The ROCOSD method. *Information Sciences, 636*, 118930.

Panayiotopoulos, C. P., Michael, M., Sanders, S., Valeta, T., & Koutroumanidis, M. (2008). Benign childhood focal epilepsies: assessment of established and newly recognized syndromes. *Brain, 131*(9), 2264-2286.

Saravanan, P., Chandra, S. S., Upadhye, A., & Gurugopinath, S. (2021). *A supervised learning approach for differential entropy feature-based spectrum sensing.* Paper presented at the 2021 Sixth International Conference on Wireless Communications, Signal Processing and Networking.

Schirmer, P. A., & Mporas, I. (2020). *Energy disaggregation from low sampling frequency measurements using multi-layer zero crossing rate.* Paper presented at the ICASSP 2020-2020 IEEE International Conference on Acoustics, Speech and Signal Processing (ICASSP).

Siuly, S., Li, Y., & Zhang, Y. (2016). EEG signal analysis and classification. *IEEE Trans Neural Syst Rehabilit Eng, 11*, 141-144.

Smith, M. C., & Hoeppner, T. J. (2003). Epileptic encephalopathy of late childhood: Landau-Kleffner syndrome and the syndrome of continuous spikes and waves during slow-wave sleep. *Journal of Clinical Neurophysiology, 20*(6), 462-472.

Topçu, Y., Kılıç, B., Tekin, H. G., Aydın, K., & Turanlı, G. (2021). Effects of sulthiame on seizure frequency and EEG in children with electrical status epilepticus during slow sleep. *Epilepsy & Behavior, 116*, 107793.

Wiwattanadittakul, N., Depositario-Cabacar, D., & Zelleke, T. G. (2020). Electrical status epilepticus in sleep (ESES)—Treatment pattern and EEG outcome in children with very high spike–wave index. *Epilepsy & Behavior, 105*, 106965.

Zhang, Y., Song, X.-f., & Gong, D.-w. (2017). A return-cost-based binary firefly algorithm for feature selection. *Information Sciences, 418*, 561-574.

Zhou, W., Zhao, X., Wang, X., Zhou, Y., Wang, Y., Meng, L., Chen, W. (2022). A hybrid expert system for individualized quantification of electrical status epilepticus during sleep using biogeography-based optimization. *IEEE Transactions on Neural Systems and Rehabilitation Engineering, 30*, 1920-1930.